

# The late-type stellar component in the ROSAT All-Sky Survey at high galactic latitude

F.-J. Zickgraf

*Hamburger Sternwarte, Gojenbergsweg 112, D-21029 Hamburg, Germany*

J.M. Alcalá and E. Covino

*Osservatorio Astronomico di Capodimonte, I-80131 Napoli, Italy*

J. Krautter and I. Appenzeller

*Landessternwarte Königstuhl, D-69117 Heidelberg, Germany*

S. Frink

*University of California San Diego, La Jolla, CA 92093-0424, USA*

M.F. Sterzik

*European Southern Observatory, Santiago 19, Chile*

**Abstract.** We investigated the properties of the late-type stellar component in the RASS at high-galactic latitude  $|b|$  based on an optically identified sample of ROSAT All-Sky Survey (RASS) X-ray sources. The stellar sample comprises  $\sim 250$  objects in six study areas covering  $685 \text{ deg}^2$  at  $|b| > 20^\circ$ . We spectroscopically detected a significant fraction of lithium-rich pre-main sequence (PMS) objects including even M-type stars. In an area located about  $20^\circ$  south of the Tau-Aur star formation region (SFR) and close to the Gould Belt, we found a large fraction of 40% PMS stars among the K-type stellar counterparts. In other areas we found a smaller but still significant fraction of Li-rich stars. We compared the  $\log N - \log S$  distribution with published galactic distribution models for different age groups and with results from the ROSAT Galactic Plane Survey. For the sample south of Tau-Aur we find an excess of PMS stars compared to model calculations while in the other areas the observed  $\log N - \log S$  is close to the model predictions. We started to investigate the proper motions and radial velocities of both, the young lithium-rich and the older stellar counterparts. Radial velocities and proper motions of the Li-rich stars in the area south of Tau-Aur are consistent with membership to the Tau-Aur SFR. The non-PMS stars show a wider spread in radial velocities and proper motions.

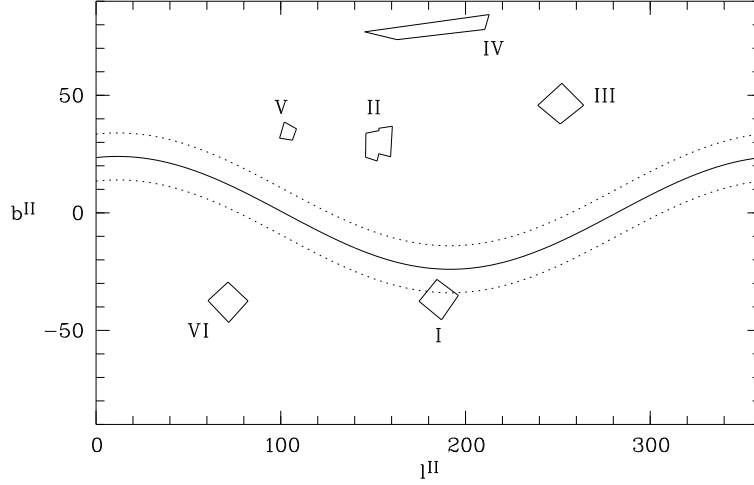


Figure 1. Distribution of the study areas in galactic coordinates. The solid and dashed lines denote the location of the Gould Belt as given by Guillout et al. (1998).

## 1. High galactic latitude sample

The optical identification of a complete sample of 674 RASS X-ray sources yielded a stellar subsample of 274 sources (Zickgraf et al. 1997, Appenzeller et al. 1998, Krautter et al. 1999). The RASS sample is distributed over six study areas located at  $|b| > 20^\circ$  and covering 685 sq. degrees (see Fig. 1). The flux limit is mostly  $1.8 \cdot 10^{-13} \text{ erg s}^{-1} \text{ cm}^{-2}$  and in the smaller area V  $6 \cdot 10^{-14} \text{ erg s}^{-1} \text{ cm}^{-2}$ . The stellar sample contains about 20% F and as much G stars, 33% K stars (with and without  $H\alpha$  emission), and 21% M stars, most of them, i.e. 90%, of type dMe.

## 2. $\log N - \log S$ distribution

The  $\log N - \log S$  distribution of the stellar sample (excluding cataclysmic variables and white dwarfs) is shown in Fig. 2. In the flux range  $S_x = 2 \cdot 10^{-13} - 1 \cdot 10^{-11} \text{ erg s}^{-1} \text{ cm}^{-2}$  the slope is  $-1.36 \pm 0.11$  calculated using a maximum-likelihood method. Below  $2 \cdot 10^{-13} \text{ erg s}^{-1} \text{ cm}^{-2}$  the distribution is even flatter with a slope of  $-1.2$ . The slope of the distribution is therefore flatter than the Euclidean slope of  $-1.5$ . It is also flatter than derived for low  $|b|$  from the Galactic Plane Survey by Motch et al. (1997) who obtained a slope of  $-1.48 \pm 0.23$  for an area in Cygnus. The deviation from the Euclidean value indicates that the stellar sample at high  $|b|$  is affected by the scale height of the galactic distribution of stellar X-ray emitters. While the average  $\log N - \log S$  is consistent with age dependent models for the space distribution of X-ray active stars by Guillout et al. (1996) for  $|b| = 30^\circ$ , area I (south of Tau-Aur) deviates as discussed already

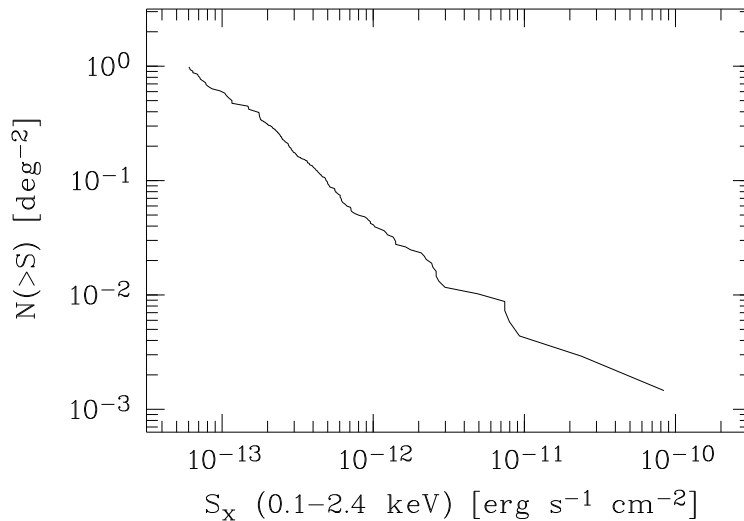


Figure 2. Combined area corrected  $\log N - \log S$  distribution of stellar counterparts (excluding cataclysmic variables and white dwarfs).

by Zickgraf et al. (1998) due to an excess of lithium-rich PMS stars (see Sect. 3.).

### 3. Lithium-rich stars

During several observing runs spectra of  $\sim 70$  G, K, and M stars have been obtained (medium and high resolution) in order to search for the Li  $\lambda 6708 \text{ \AA}$  absorption line. The results are summarized in Tab. 1. Equivalent widths have been converted to abundances using the curves of growth by Pavlenko & Magazzú (1996). So far, in 15 of 67 K stars strong lithium lines have been found. Most of them, i.e. eight K stars, are located in area I which contains 20 K and Ke stars. In areas II, III, and VI 7 of 47 K and Ke stars exhibit strong Li-absorption lines. Even 2 of 40 M stars show very strong lithium lines, one in area I and the other one in area II. Whereas the survey in 4 of the 6 areas is complete for the K and M stars, it is not yet complete for the G stars. However, three G stars in area I exhibit strong lithium, and three further G stars have considerable Li-absorption. In area VI one of three G stars observed so far exhibits considerable Li-absorption.

### 4. Proper motions and radial velocities

We searched the HIPPARCOS, TYCHO, PPM, STARNET (Röser 1996), and ACT (Urban et al. 1997) catalogs for the stars in our sample in order to obtain proper motions. Figure 3 shows the proper motions and the respective vectors of motion for area I. The Li-rich stars have proper motions clustering in a smaller range than stars without significant lithium. The two lithium-rich stars in the lower right corner of the left panel of Fig. 3 deviating in proper motion are

V774 Tau and V891 Tau. They also have a different direction of motion and different radial velocities (cf. Fig. 4) and possibly belong to the UMa cluster at a distance of about 20 pc.

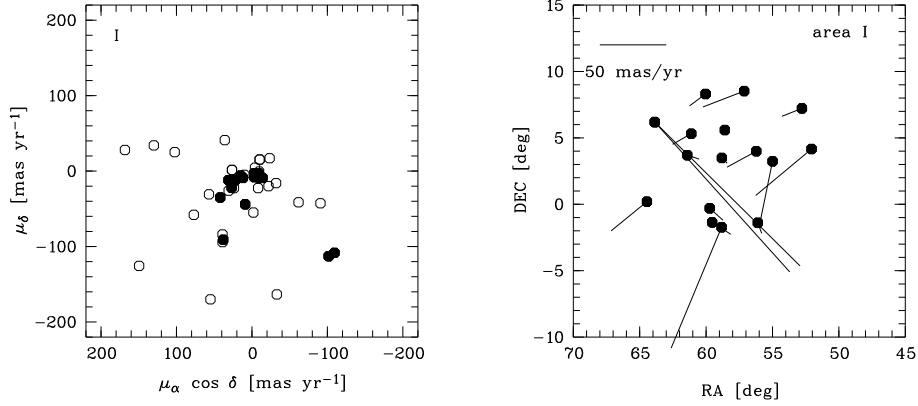


Figure 3. Proper motions (left panel) and projected directions of motion (right panel) for stellar X-ray emitters in area I. Filled symbols: Li-rich stars. Open symbols: stars with  $W(\text{Li}) < 50 \text{ m}\text{\AA}$ .

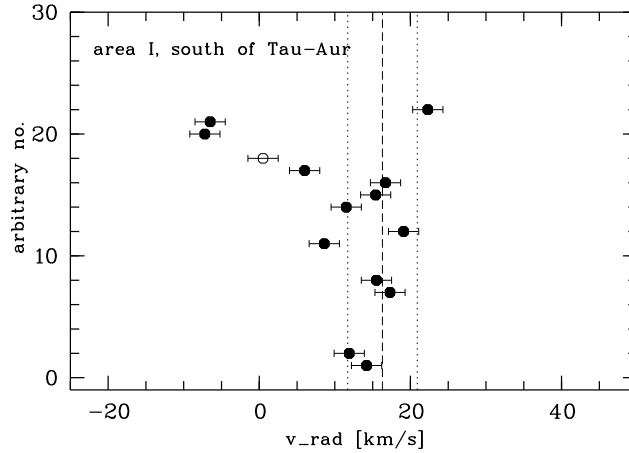


Figure 4. Heliocentric radial velocities for area I. Filled symbols: lithium-rich stars, open symbols: stars without lithium. The velocity range of Tau-Aur is marked by long and short dashed lines.

The heliocentric radial velocities measured for stars in area I are shown in Fig. 4. For most Li-rich stars the radial velocity (RV) is close to the mean RV for the Taurus T Tauri stars of  $16\text{--}17 \text{ km s}^{-1}$ . The mean and range of the RV measured by Neuhäuser et al. (1997) for PMS stars south of Taur-Aur are displayed as long and short dashed lines, respectively. These stars are probably located at a mean distance of  $\sim 140 \text{ pc}$ . The two stars with the lowest  $v_{\text{rad}}$  are the same as mentioned above.

Zickgraf et al. (1998) estimated an age of  $\sim 30 \text{ Myr}$  for the lithium-rich stars in area I. The proper motions and radial velocities suggest that they form

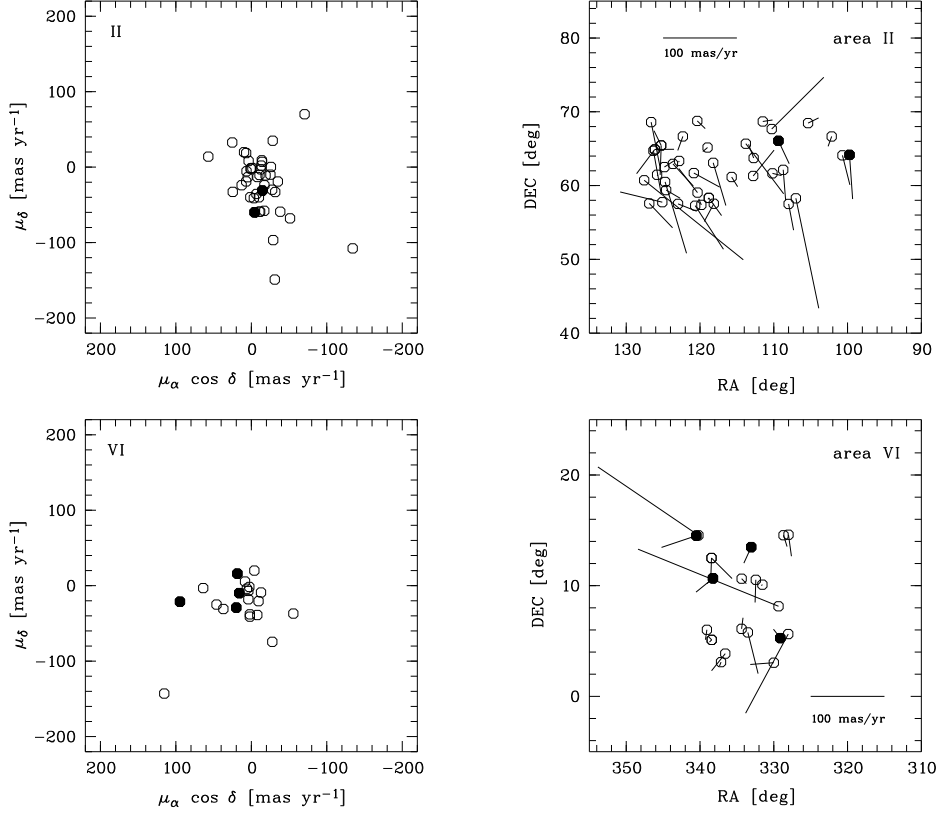


Figure 5. Proper motions and projected directions of motion for area II and VI. Filled symbols: Li-rich stars.

a kinematically rather homogenous group consistent with their young age (cf. also Frink et al. 1997).

Preliminary results of the investigation of proper motions in the other areas are shown in Fig.5. In area II the Li-rich stars seem to follow the general trend in proper motion. In area VI three of the four Li-rich stars move in the same direction whereas for the other stars no clear pattern is discernible. The scatter of the proper motions is different for each study area. Areas II and V have the smallest scatter ( $30 - 50 \text{ mas yr}^{-1}$ ), area III with  $\sim 150 \text{ mas yr}^{-1}$  the largest.

## References

- Appenzeller, I., Thiering, I., Zickgraf, F.-J., et al., 1998, ApJS, 117, 319  
 Frink, S., Röser, S., Neuhäuser, R., Sterzik, M.F., 1997, A&A, 325, 613  
 Guillout, P., et al., 1996, A&A 316, 89  
 Guillout, P., Sterzik, M.F., Schmitt, J.H.M.M., et al. 1998, A&A 334, 540  
 Krautter, J., Zickgraf, F.-J., Appenzeller, I., 1999, A&A, in press  
 Motch, C., Guillout, P., Haberl, F., et al., 1997, A&A 318, 133

Table 1. Lithium equivalent widths and abundances for G, K and M stars (on the usual scale of  $\log N(\text{H}) = 12$ ) with  $W(\text{Li}) > 50 \text{ m}\text{\AA}$ . Estimated uncertainties of the abundances are about 0.3-0.4 dex. Sequence number refer to Appenzeller et al. (1998). F015 is a binary system. Both components show Li I absorption.

Sequ. #	ROSAT name	Sp. type	$W(\text{Li})[\text{m}\text{\AA}]$	$\log N(\text{Li})$
A001	RX J0328.2 + 0409	K0	180	+2.6
A010	RX J0331.1 + 0713	K4e	410	+2.9
A042	RX J0339.9 + 0314	K2	140	+2.0
A057	RX J0344.4 – 0123	G9	290	+3.1
A058	RX J0344.8 + 0359	K1e	250	+2.7
A071	RX J0348.9 + 0110	K3(e)	250	+2.3
A094	RX J0355.2 + 0329	K3e	350	+2.7
A095	RX J0355.3 – 0143	G5	230	+3.1
A100	RX J0358.1 – 0121	K4e	310	+2.4
A101	RX J0358.9 – 0017	K3e	265	+2.4
A104NE	RX J0400.1 + 0818	G5	315	+3.5
A126	RX J0405.6 + 0341	G0	70	+2.7
A144	RX J0412.1 + 0044	G0	60	+2.6
A151NW	RX J0415.4 + 0611	G0	60	+2.6
A151SE	RX J0415.4 + 0611	G0	80	+2.7
A161	RX J0417.8 + 0011	M0e	380	+1.7
B002	RX J0638.9 + 6409	K2	255	+2.5
B039	RX J0717.4 + 6603	K3e	200	+2.2
B206	RX J0828.1 + 6432	M1e	620	+2.3
C176	RX J1059.7 – 0522	K1	170	+1.8
C200	RX J1105.3 – 0735	K5e	100	+1.3
F015	RX J2156.4 + 0516	K2	140/190	+2.0/+2.3
F046	RX J2212.2 + 1329	G5	110	+2.6
F101	RX J2232.9 + 1040	K2	190	+2.3
F140	RX J2241.9 + 1431	K0	300	+3.0

Neuhäuser, R., et al., 1997, A&A, 325, 647

Pavlenko, Ya.V., Magazzú, A., 1996, A&A 311, 961

Röser, S., 1996. In: Ferraz-Mello S., Morando B., Arlot J.-E., (eds.), Kluwer, Dordrecht, p. 481

Urban, S.E., Corbin, Th.E., Wycoff, G.L., 1997. The ACT reference catalogue, U.S. Naval Observatory, Washington, D.C

Zickgraf, F.-J., Thiering, I., Krautter, J., et al., 1997, A&AS 123, 103

Zickgraf, F.-J., Alcalá, J.M., Krautter, J., et al., 1998, A&A 339, 457